Fully relativistic spin-polarized description of magnetic interface coupling: Fe multilayers in Au(100)

L. Szunyogh
Institut für Technische Elektrochemie, Technische Universität Wien, Getreidemarkt 9/158, A-1060, Wien, Austria and Institute of Physics, Technical University Budapest, Budafoki út 8, H-1521, Budapest, Hungary

B. Újfalussy and P. Weinberger
Institut für Technische Elektrochemie, Technische Universität Wien, Getreidemarkt 9/158, A-1060, Wien, Austria

C. Sommers
Laboratoire de Physique des Solides, Bat. 510, Campus d'Orsay, 91 405 Orsay, France
(Received 18 October 1995; revised manuscript received 10 May 1996)

The spin-polarized fully relativistic screened Korringa-Kohn-Rostoker method is applied to calculate magnetic interface coupling energies (MICE's) for Fe multilayers in Au(100), separated by up to 16 spacer layers of Au. With respect to the antiparallel as well as to a perpendicular relative orientation of the magnetization in the Fe slabs the MICE's as calculated (a) in terms of total energies, (b) within the force theorem approximation, and (c) within the frozen potential approximation are discussed using the concept of layer-resolved quantities. In particular the comparison between the total energy and the force theorem approach is presented in some detail because of possible implications for an *ab initio* description of transport properties in multilayer systems. [S0163-1829(96)01733-X]

I. INTRODUCTION

An experimental study of magnetic interface coupling typically is based on a sample setup consisting of a magnetic whisker as a substrate, a nonmagnetic spacer wedge, and a magnetic overlayer, whereby the whisker can also be replaced by a reasonably thick layer of a magnetic metal well grown on a suitable substrate and the magnetic overlayer can have a cap. Scanning the thickness of the wedge and measuring simultaneously, for example, the orientation of the magnetic field in the magnetic overlayer eventually shows the by-now famous oscillations for the orientation of the magnetic field. For example for Fe/Au/Fe multilayers it was found[1] that the orientation of the magnetization is in the plane of the overlayer and that by fitting the observed oscillations to a model for bilinear coupling two periods of oscillations could be extracted. Quite clearly, possible surface reconstructions and different growing conditions do matter; however, at least the periods of oscillations seem to be quite reproducible.

In order to describe theoretically the magnetic interface coupling (see, e.g., Ref. 2 and references therein), three main aspects should be observed: Namely, (1) the experimental measurements are performed only for truely semi-infinite systems, (2) microscopic interdiffusion and macroscopic roughness can occur, and last but not least (3) in principle the actual orientation of the magnetization has to be taken into account. The first aspect implies that for any system under consideration (at best) only two-dimensional translational invariance applies. The second aspect invokes in particular experimental guidance, since at least typical concentration profiles in the vicinity of the occurring interfaces are needed. Nevertheless, theoretical studies to describe the effect of surface roughness are already on the way.[3] It is now generally accepted that in the asymptotic limit the experimentally observed oscillatory behavior of the coupling is governed by the spacer Fermi surface.[4] But there still remain a few questions concerning the role of relative orientations, sometimes referred to as ''biquadratic coupling.''[5] This aspect, however, is of purely theoretical nature: Only in a (fully) relativistic description can an orientation of the magnetization be defined. There is also little known about other physical quantities — like charges, induced moments, etc. — in the limit of small spacer thicknesses, which in turn might be of crucial importance for transport properties. Quite clearly a study of these properties requires self-consistent calculations and an analysis of corresponding results to frozen potential and force theorem calculations frequently found in the literature.

In the present paper the spin-polarized fully relativistic screened Korringa-Kohn-Rostoker (KKR) method for two-dimensional translational-invariant systems[6] is applied in order to calculate magnetic interface coupling energies (MICE's) for Fe multilayers in Au(100) corresponding to antiparallel and to perpendicular global orientations of the magnetization in the Fe layers separated by Au spacer layers. Particular emphasis will be given to ''traditional'' approximations for the MICE's such as the frozen potential approximation and the force theorem approximation, and their possible implications for transport properties.

II. THEORETICAL CONSIDERATIONS

In general, in a relativistic spin-polarized multiple scattering theory the system is described by an effective Kohn-Sham-Dirac Hamiltonian[7,8]

$$\mathcal{H}(\mathbf{r}) = c\,\boldsymbol{\alpha}\cdot\mathbf{p} + \beta mc^2 + I_4 V(\mathbf{r}) + \beta\boldsymbol{\sigma}\cdot\mathbf{B}^{\mathrm{eff}}(\mathbf{r}), \qquad (1)$$

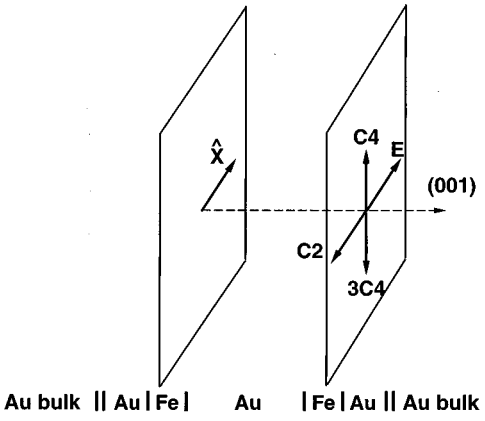

FIG. 1. The interface region and orientation of the magnetization.

where the α_i $(i=1,2,3)$ and β are Dirac matrices, σ_i $(i=1,2,3)$ Pauli matrices, I_4 is a 4×4 unit matrix, and $V(\mathbf{r})$ and $\mathbf{B}^{\text{eff}}(\mathbf{r})$ usually are chosen to be of muffin-tin form[8]

$$V(\mathbf{r})=\sum_i V_i(\mathbf{r}_i), \quad V_i(\mathbf{r}_i)=\begin{cases} V_i(r_i), & r_i\leqslant S_i, \\ \text{const}, & \text{otherwise}, \end{cases} \tag{2}$$

$$\mathbf{B}^{\text{eff}}(\mathbf{r})=\sum_i \mathbf{B}_i^{\text{eff}}(\mathbf{r}_i), \quad \mathbf{B}_i^{\text{eff}}(\mathbf{r}_i)=\begin{cases} \mathbf{B}_i^{\text{eff}}(r_i), & r_i\leqslant S_i, \\ \text{const}, & \text{otherwise}, \end{cases} \tag{3}$$

$$\mathbf{B}_i^{\text{eff}}(r_i)=B_i^{\text{eff}}(r_i)\hat{\mathbf{e}}_i. \tag{4}$$

Here the $\mathbf{R}_i$ specify the positions of the scattering sites, $\mathbf{r}_i=\mathbf{r}-\mathbf{R}_i$, $r_i=|\mathbf{r}_i|$, S_i is the corresponding muffin-tin radius, and the sum extends over all scattering sites i. For a chosen set of orientations $\{\hat{\mathbf{e}}_i\}$ the potentials $V_i(r_i)$ and effective exchange fields $B_i^{\text{eff}}(r_i)$ are determined self-consistently and the total energies are then compared to each other. A direction $\hat{\mathbf{e}}_i$ can be given, e.g., by the direction of the corresponding in-plane projection $\hat{\mathbf{e}}_{i,\parallel}$ and by an azimuthal angle θ_i defining the projection onto the z axis (normal to the planes). Furthermore, by choosing an in-plane vector $\hat{\mathbf{n}}$, a rotation around the z axis, R_i, can be defined for each layer i such that $\hat{\mathbf{e}}_{i,\parallel}=R_i\hat{\mathbf{n}}$.[9] Consequently, $\{\hat{\mathbf{e}}_i\}$ is uniquely characterized by the symbol

$$\{\hat{\mathbf{n}};(R_1,\theta_1),(R_2,\theta_2),(R_3,\theta_3),\ldots\}. \tag{5}$$

It should be emphasized that the very weak dependence of physical quantities on the choice of $\hat{\mathbf{n}}$ is usually referred to as magnetocrystalline anisotropy.

Figure 1 describes the particular geometrical setup in the present calculations. As one can see there are three regions. The left and right ones are semi-infinite with all physical properties identical to those of bulk Au. The intermediate region is further partitioned into a left and a right part such that each of these individual parts contains n layers of Fe, whereby the two Fe slabs are separated by m layers of Au, often referred to as the ''spacer.'' The spacer layers are then attributed symmetrically to the left (right) Fe slab to form the left (right) part of the intermediate region. In order to treat the outer interfaces realistically, a buffer of a few Au layers (two in the present calculations) between the left (right) Fe slab and the corresponding left (right) semi-infinite Au was included in the intermediate region. Throughout this paper only in-plane $(\theta_i=0,\forall i)$ orientational configurations are considered with the *particular choice* of $\hat{\mathbf{n}}=\hat{\mathbf{x}}$. Keeping the orientations in the left part of the interface region uniformly fixed to $\hat{\mathbf{x}}=E\hat{\mathbf{x}}$, where E denotes the identity rotation, and specifying a uniform in-plane orientation in the right part of the intermediate region (see Fig. 1):

$$\{\hat{\mathbf{x}};E,E,\ldots,E,R,R,\ldots,R\}, \tag{6}$$

a particular orientational configuration can be labeled simply by R. For the present case of a (100) interface of a parent fcc lattice (one atom per unit cell) we considered the cases $R=E$, C_4^+, and C_2. Quite clearly, $R=C_4^-$ would display a situation identical to $R=C_4^+$. In the spirit of the above, a label E refers to a ferromagnetic configuration; i.e., both in the left and the right halves of the intermediate region the magnetization is pointing along the x-axis, a label C_2 to an antiparallel and label C_4^+ to a perpendicular configuration.

In order to calculate the magnetic interface coupling energy (MICE's), namely, the energy difference between a particular configuration R and the ferromagnetic one, three levels of sophistication can be applied; all three of them are more or less frequently used in the by-now vast literature on magnetic interface coupling. It should be noted that for in-plane orientations of the magnetization as in the present case of a fcc (100) interface no contributions to the MICE's due to magnetostatic dipole-dipole interactions arise.[6]

A. Total energy calculations

Let $\Delta\epsilon_i(R)$ denote the following difference of layer-resolved total energies for a given arrangement of n layers of Fe and m layers of the spacer:

$$\Delta\epsilon_i(R)=\epsilon_i(R)-\epsilon_i(E), \tag{7}$$

where i specifies a particular layer; then the MICE $\Delta\epsilon(R)$ for a given configuration (R) is given by a summation over all layers in the interface region:

$$\Delta\epsilon(R)=\sum_i \Delta\epsilon_i(R). \tag{8}$$

The advantages of a direct calculation of the MICE in terms of total energies are obvious; namely, simultaneously one obtains correct layer-resolved charges and magnetic moments (charge densities and magnetization densities), which can be of quite some importance for a description of physical properties other than the MICE such as, for example, transport properties. Furthermore, the MICE can formally be partitioned into contributions arising from the magnetic layers, the spacer, and the buffer (see also Fig. 1),

$$\Delta\epsilon(R)=\Delta\epsilon^{\text{Fe}}(R)+\Delta\epsilon^{\text{spacer}}(R)+\Delta\epsilon^{\text{buffer}}(R). \tag{9}$$

Unfortunately the disadvantage of this kind of approach is also obvious: Calculations tend to be extremely lengthy.

B. Force theorem approximation

Suppose for one particular arrangement of n layers of Fe and m layers of the spacer the layer-dependent potentials $V_i(r_i)$ and effective fields $B_i^{\text{eff}}(r_i)$ are calculated self-consistently for the ferromagnetic configuration (E); then the MICE is approximated within the force theorem approximation as the following difference of band energies (see, e.g., Ref. 6):

$$\Delta\epsilon(R)\approx\Delta\epsilon^{\text{FT}}(R)=\epsilon^{\text{band}}(R)-\epsilon^{\text{band}}(E), \tag{10}$$

such that

$$\left.\begin{aligned} V_i(r_i;R)&=V_i(r_i;E)\\ B_i^{\text{eff}}(r_i;R)&=B_i^{\text{eff}}(r_i;E)\end{aligned}\right\}\forall i. \tag{11}$$

If the band energy is not calculated using the Lloyd formulation for the integral density of states, but in terms of layer-resolved densities of states, then also $\Delta\epsilon^{\text{FT}}(R)$ can be split up into contributions from the spacer and from the magnetic slabs.

C. Frozen potential approximation

Within the frozen potential approximation the MICE is again defined in terms of the differences of band energies,

$$\Delta\epsilon(R)\approx\Delta\epsilon^{\text{FP}}(R)=\epsilon^{\text{band}}(R)-\epsilon^{\text{band}}(E); \tag{12}$$

however, the layer-dependent potentials in the interface region are constructed by replacing the potentials of the spacer by the corresponding bulk potential and using an *ad hoc* potential for the layers corresponding to the magnetic slabs; i.e., for the system under consideration,

$$V_i(r_i;R)=V_i(r_i;E)\equiv\begin{cases}V^{\text{bulk}}(r_i), & i\in\text{spacer},\\ V^{\text{Fe}}(r_i), & i\in\text{Fe multilayer},\end{cases} \tag{13}$$

$$B_i^{\text{eff}}(r_i;R)=B_i^{\text{eff}}(r_i;E)\equiv\begin{cases}0, & i\in\text{spacer}\\ B^{\text{Fe}}(r_i), & i\in\text{Fe multilayer}.\end{cases} \tag{14}$$

In the present calculations whenever the frozen potential approximation is used, $V^{\text{Fe}}(r)$ and $B^{\text{Fe}}(r)$ are the potential and effective fields of a single layer of Fe in Au(100), while $V^{\text{bulk}}(r)$ is the fcc bulk potential of Au. Frequently the potentials in the magnetic slabs are simply constructed by using a bulk potential of the magnetic metal adjusted to the Fermi level of the bulk metal corresponding to the spacer.

III. COMPUTATIONAL DETAILS

The spin-polarized relativistic version[6] of the screened Korringa-Kohn-Rostoker (KKR) method,[10,11] was used self-consistently within the local spin density approximation (LSD) and the atomic sphere approximation (ASA). Energy integrations were performed along a semicircular contour using a 15-point Gaussian sampling on an asymmetric (logarithmic) mesh. All values of $\Delta\epsilon^{\text{FT}}(R)$ and $\Delta\epsilon^{\text{FP}}(R)$, if not stated differently, correspond to lattice Fourier transformations using 325 $k_\parallel$ points in the irreducible wedge of the surface Brillouin zone, while all values of $\Delta\epsilon(R)$, if not specified differently, refer to a mesh of 45 $k_\parallel$ points. The parent fcc lattice corresponds to a lattice constant of 7.6813 a.u. (bulk Au).

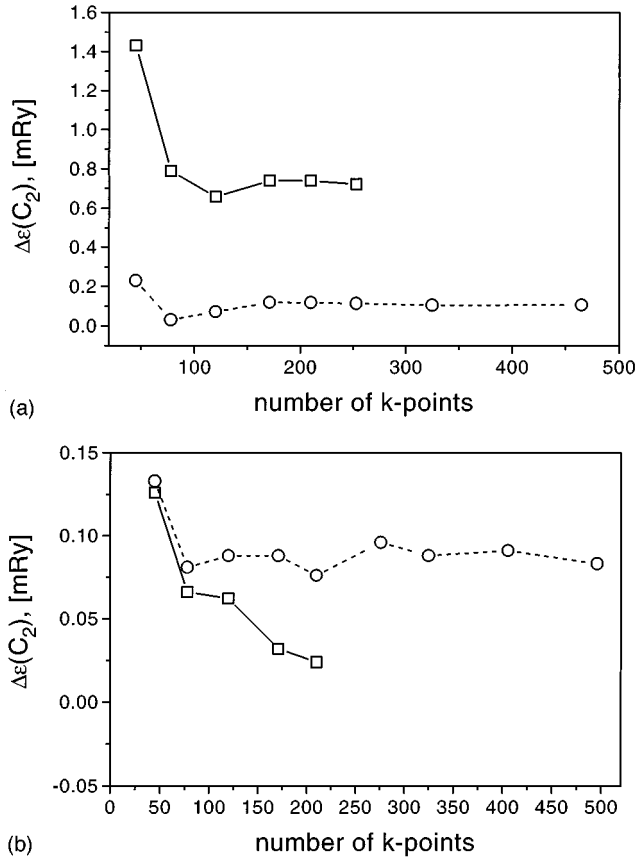

FIG. 2. Convergence of the MICE $\Delta\epsilon(C_2)$ with respect to the number of $k_\parallel$ points used: single layers of Fe separated by (a) three layers of Au and (b) nine layers of Au. Squares, total energy calculation; circles, force theorem calculation [$\Delta\epsilon^{\text{FT}}(C_2)$].

IV. RESULTS

Figure 2 shows the convergence of the MICE $\Delta\epsilon(C_2)$ and $\Delta\epsilon^{\text{FT}}(C_2)$ with respect to the number of $k_\parallel$ points used in the irreducible wedge of the surface Brillouin zone for two different cases, namely, for single layers of Fe separated by (a) three layers of Au and (b) nine layers of Au. The first case corresponds to a system with a thin spacer, while the second is representative for a system with a medium thickness of the spacer. These two systems were in particular investigated in all necessary details, since they also bracket situations of large and small MICE's. Inspecting first Fig. 2(a), one can see that $\Delta\epsilon(C_2)$ and $\Delta\epsilon^{\text{FT}}(C_2)$ are well converged; however, $\Delta\epsilon^{\text{FT}}(C_2)$ is by about a factor of 7 smaller than $\Delta\epsilon(C_2)$. This indeed is not surprising, since for thin spacers the effect of self-consistency has to be expected to be much larger than for thick spacers. Fig. 2(b) illustrates that in the case of small MICE's [$\Delta\epsilon(C_2),\Delta\epsilon^{\text{FT}}(C_2)<$ 0.1 mRy] the $k_\parallel$ convergence is a much more subtle problem. It is rather reassuring that on the average $\Delta\epsilon(C_2)$ differs from $\Delta\epsilon^{\text{FT}}(C_2)$ by less than about 0.05 mRy. As compared to the converged value of $\Delta\epsilon^{\text{FT}}(C_2)$, the value of $\Delta\epsilon(C_2)$ as calculated using only 45 $k_\parallel$ points gives a reasonably good ac-

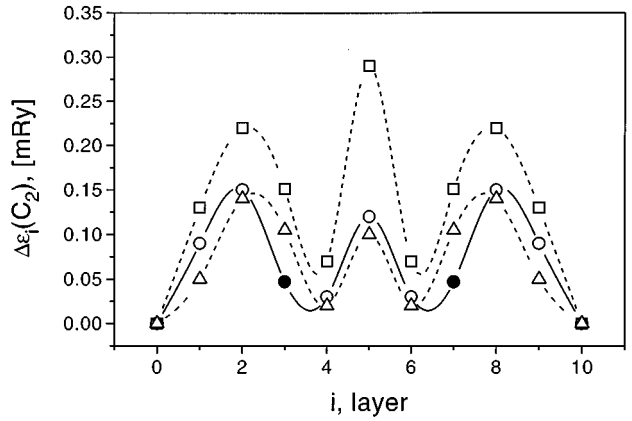

FIG. 3. Convergence of the layer-resolved MICE $\Delta\epsilon_i(C_2)$ with respect to the number of k points used for singles layers of Fe separated by three layers of Au. Squares, 45; triangles, 171; circles, 253 $k_\parallel$ points. The positions of the Fe layers are marked as solid symbols.

count for the MICE. This in turn shows that $\Delta\epsilon(R)$ values based on the use of a minimal grid of 45 $k_\parallel$ points provide at least a convincing qualitative correct behavior.

In Fig. 3 the layer-resolved MICE's, $\Delta\epsilon_i(C_2)$ corresponding to differently dense $k_\parallel$ grids are displayed for the case of single layers of Fe separated by three layers of Au. As one can see the minimal grid results give a qualitatively correct behavior, namely, that there are peaks corresponding to the central layer of the interface region and to the buffer layer neighboring the Fe layers. Summing over all corresponding $\Delta\epsilon_i(C_2)$ values then yields the values of $\Delta\epsilon(C_2)$ shown in Fig. 2(a). Quite clearly, the layer resolution as shown in Fig. 3 gives a very detailed description of the MICE.

In order to show the oscillatory behavior of the MICE with respect to increasing spacer thickness, in Fig. 4(a) $\Delta\epsilon^{\mathrm{FP}}(R)$, $R=C_2, C_4^+$ [see Eqs. (8) and (9)] is shown for single layers of Fe, separated by m layers of Au. For $R=C_2$ we also cross-checked the results of the fully relativistic calculations with the predictions of a scalar relativistic theory. As expected, the MICE from both approaches [see open and solid squares in Fig. 4(a)] compare well to each other, supporting the common believe that the MICE is mainly governed by the nonrelativistic exchange coupling, while additional effects related to relativity, i.e., spin-orbit coupling, play a minor role only. To confirm this we also investigated the dependence of the MICE with respect to the choice of $\hat{\mathbf{n}}$ [see Eq. (5) and the comment below] and found that as compared to the case of $\hat{\mathbf{n}}=\hat{\mathbf{x}}$ differences in corresponding MICE are within the present accuracy of calculating magnetic anisotropy energies; i.e., changes in the MICE caused by a different choice of $\hat{\mathbf{n}}$ are of the order of 5%.

As can be seen from this figure, $\Delta\epsilon^{\mathrm{FP}}(R)$ is distinctly negative for $m=5,8,10,13,15$. These peaks are exactly at positions seen in the experiment[1] for Fe/Au/Fe multilayers. A short period of about 2.5 layers, which was found theoretically also by Bruno and Chappert,[12] can be directly read off from Fig. 4(a). It is also apparent from Fig. 4(a) that the amplitudes corresponding to a perpendicular arrangement (C_4^+) are in general smaller than those corresponding to an

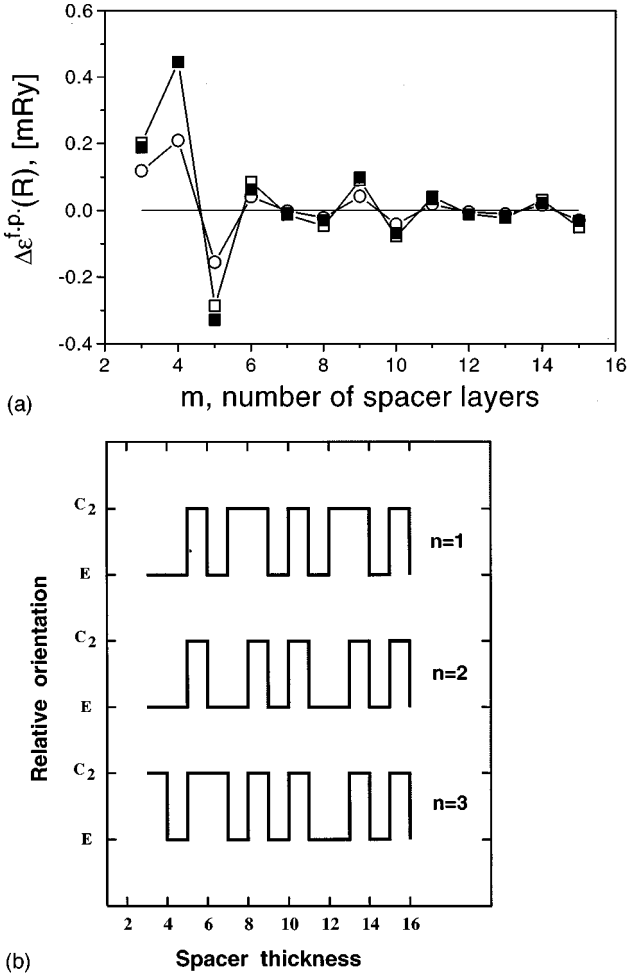

FIG. 4. (a) Frozen potential calculations of the MICE ($\Delta\epsilon^{\mathrm{FP}}(R)$) with respect to the spacer thickness m single layers of Fe. Open squares: C_2 fully relativistic approach; full squares: C_2 scalar relativistic approach; circles: C_4^+ fully relativistic approach. (b) Frozen potential calculations: preferred relative orientation of the magnetization as a function of spacer thickness for single, double, and triple layers of Fe.

antiparallel alignment (C_2). This implies that the ground state of the system corresponds either to a parallel or an antiparallel relative orientation of the magnetic field. Figure 4(b) illustrates the preferred relative orientation as a function of spacer thickness and for different numbers of Fe layers. In principle Fig. 4(b) can be directly compared to experimental data.[1]

Of considerable theoretical interest is the relation of the frozen potential approximation with respect to the force theorem approximation and a direct calculation of MICE in terms of total energies. In order to illustrate the regimes of applications of these three approaches, in Fig. 5 the MICE differences

$$\Delta E(R)=\begin{cases}\Delta\epsilon^{\mathrm{FP}}(R)-\Delta\epsilon^{\mathrm{FT}}(R),\\ \Delta\epsilon^{\mathrm{FP}}(R)-\Delta\epsilon(R)\end{cases} \tag{15}$$

are shown with respect to a restricted number of spacer layers for single, double, and triple layers of Fe. As one can see from Fig. 5(a), for single layers the force theorem approxi-

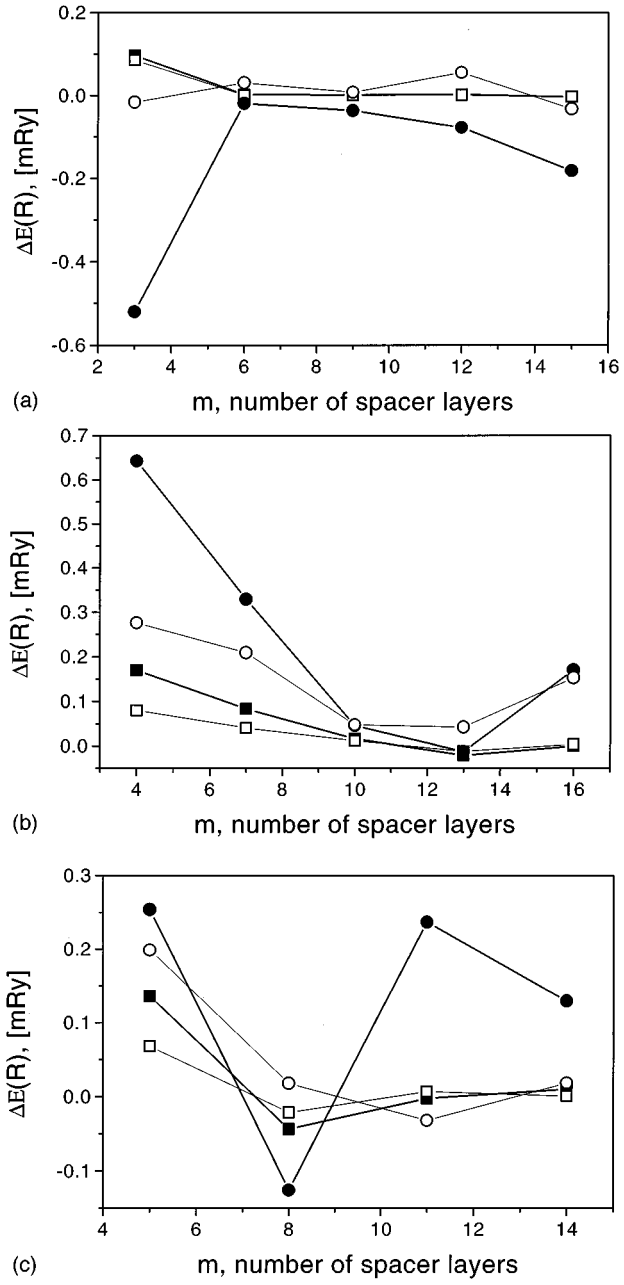

FIG. 5. Difference of the MICE with respect to the frozen potential calculations, $\Delta E(R)$, for (a) single layers, (b) double layers, and (c) triple layers. Squares, force theorem; circles, total energy calculation; solid symbols, C_2; open symbols, C_4^+.

mation becomes virtually identical to the frozen potential approximation for $m>6$. For double and triple layers of Fe [see Figs. 5(b) and 5(c)] this seems to be the case for $m>10$. Rather interesting is the behavior of $\Delta E(R)$ for single and in particular for triple layers for $m>10$, since for $R=C_4^+$ the total-energy-related values show about the same deviations from the frozen potential approximation as the force theorem (FT) values, while for $R=C_2$ the deviations are of the order of about 0.1 mRy. Inspecting Fig. 5(b) only, one might argue that for $m=16$ the $k_\parallel$ integration starts to become insufficient, which, however, in view of the C_4^+ results for single and triple layers of Fe is unlikely to be the case.

TABLE I. Component-resolved contributions to the MICE [mRy] for $Fe_nAu_mFe_n(001)$ multilayers. The first line corresponds to C_2, the second line to C_4^+. For comparison the total MICE as obtained by means of the force theorem is also listed.

n	m	Fe	Spacer	Buffer	FT	Layers
1	3	0.302	0.430	0.700	0.105	9
		0.064	-0.010	0.080	0.033	
1	6	-0.116	0.200	0.020	0.083	12
		-0.050	0.060	0.000	0.04	
1	9	0.116	0.030	-0.020	0.088	15
		0.094	-0.020	-0.040	0.042	
1	12	0.017	0.050	0.000	-0.014	18
		-0.011	-0.040	-0.010	-0.007	
1	15	-0.010	0.120	0.020	-0.049	21
		-0.028	0.030	0.000	-0.028	
2	1	-0.100	-0.020	-0.540	-0.327	9
		-0.022	0.010	-0.190	-0.132	
2	4	0.404	0.080	-0.220	0.577	12
		0.148	0.060	-0.040	0.278	
2	7	-0.006	-0.150	0.040	-0.034	15
		-0.002	-0.090	0.000	-0.012	
2	10	-0.158	0.020	0.020	-0.090	18
		-0.092	-0.020	0.000	-0.050	
2	13	0.037	-0.080	-0.040	-0.010	21
		0.034	-0.060	-0.060	-0.004	
2	16	-0.070	-0.080	0.000	0.018	24
		-0.024	-0.120	0.020	0.007	
3	2	-0.658	-0.300	0.220	-1.034	12
		-0.302	-0.180	0.110	-0.498	
3	5	-0.217	-0.390	0.000	-0.552	15
		-0.152	-0.230	0.040	-0.283	
3	8	-0.079	0.080	0.010	0.009	18
		-0.045	0.000	-0.010	0.009	
3	11	0.024	-0.140	0.020	0.076	21
		0.038	0.050	-0.020	0.031	
3	14	0.004	-0.080	0.000	0.023	24
		0.012	0.000	-0.020	0.014	

From Table I, listing componentlike contributions to the MICE, it is obvious that for $R=C_2$ in the case of single layers of Fe for $m>12$ the contribution from the spacer is increasing quite a bit, while the contribution from the Fe layers is only slightly decreasing. For triple layers of Fe Table I reveals that for $R=C_2$ the contribution of the spacer starts to oscillate for $m>8$, which in turn gives rise to the peculiar shape of the corresponding difference curve in Fig. 5(c). For double layers at $m=16$, both contributions, namely, from the Fe layers and the spacer, seem to matter. Table I is also interesting for two further reasons; namely (i) one clearly can read off from the buffer contribution the importance of the outer interfaces for systems with thin spacers and (ii) for a variety of systems the importance of the spacer contribution to the MICE is documented in a consistent manner. It should be recalled that all values in this table refer to a mesh of 45 $k_\parallel$ points.

In order to discuss these componentlike contributions in a more quantitative way, in Fig. 6 their convergence with respect to the applied $k_\parallel$ mesh is shown for single layers of Fe

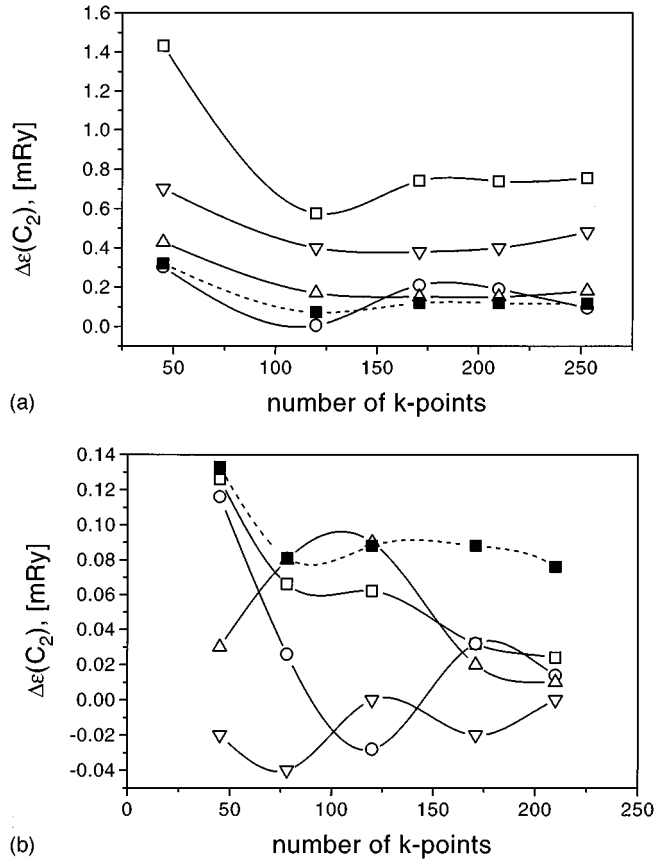

FIG. 6. Convergence of the componentlike contributions of the MICE $\Delta\epsilon(C_2)$ with respect to the number of $k_\parallel$ points: single layers of Fe separated by (a) three layers of Au and (b) nine layers of Au. Squares, total MICE; circles, Fe contribution; up-triangles, Au spacer contribution; down-triangles, Au buffer contribution. For a comparison also $\Delta\epsilon^{\mathrm{FT}}(C_2)$ is shown (solid squares).

separated by three and by nine layers of Au. From Fig. 6(a) one can see that although the MICE's $\Delta\epsilon(C_2)$ is well converged, the difference between the last two values being less than 0.020 mRy, there are still changes in the Fe contribution, which are mostly compensated by respective changes in the buffer contribution. The shape of $\Delta\epsilon(C_2)$ as a function of the $k_\parallel$ mesh clearly resembles that of the Fe contribution. For the case of nine spacer layers [Fig. 6(b)], the changes in the Fe contribution are mostly compensated by opposite changes in the spacer contribution. The differently shaped oscillations in the componentlike contributions are obviously also the main reason for the rather ''bumpy'' convergence of $\Delta\epsilon^{\mathrm{FT}}(C_2)$ in Fig. 2(b). From Fig. 6(a) one safely can conclude that (1) the biggest contribution arises from the buffer and (2) the contributions from the Fe layers and the spacer layers are about the same. For large enough $k_\parallel$ points the contributions from the Fe layers and the spacer layers to the MICE of the nine-spacer-layer system are again about the same while the contribution from the buffer is smaller. It should be noted that in the case of nine spacer layers $\Delta\epsilon(C_2)$ is an order of magnitude smaller than in the case of three spacer layers.

While MICE and even the componentlike contributions to these energies are basically global quantities, layer-resolved quantities offer a remarkable characterization of the difference between the force theorem approximation and the total energy approach. In Fig. 7 the $\Delta\epsilon_i(R)$'s and the corresponding differences for the charges and magnetic moments,

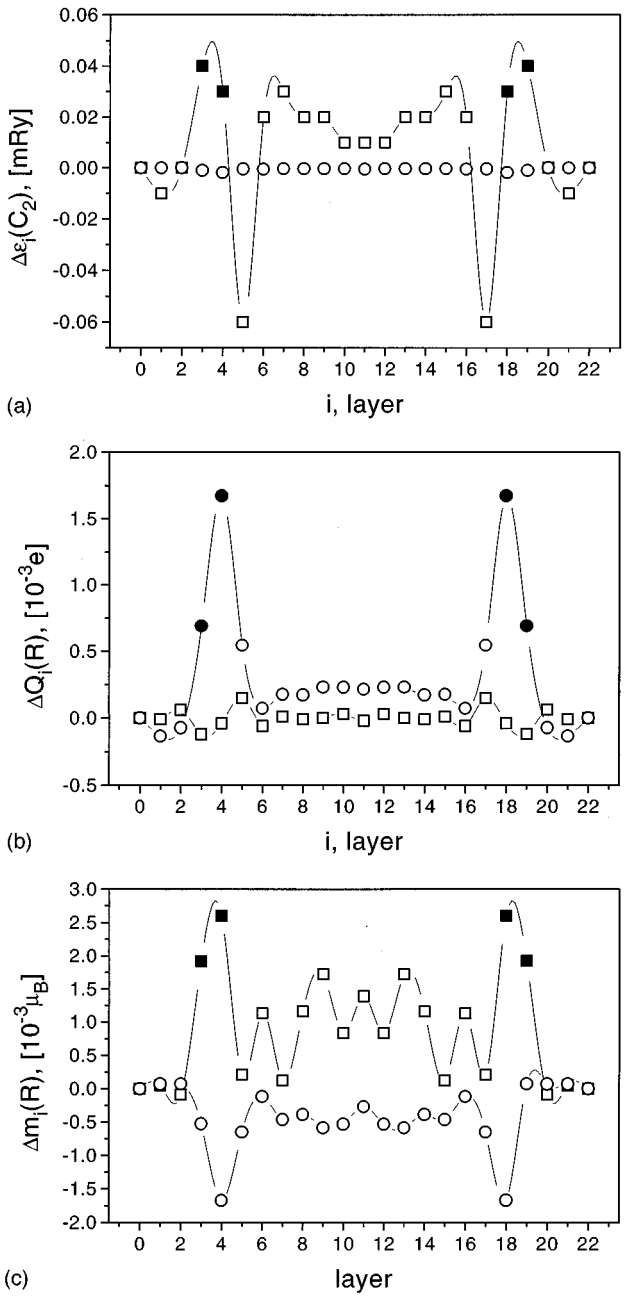

FIG. 7. Layer-resolved differences with respect to the ferromagnetic orientation for the case of double layers of Fe separated by 13 layers of Au: (a) total energies, (b) charges, and (c) magnetic moments. Squares, total energy calculation; circles, force theorem. The positions of the Fe layers are marked as solid symbols.

$$\Delta Q_i(R) = Q_i(R) - Q_i(E), \tag{16}$$

$$\Delta m_i(R) = m_i(R) - m_i(E), \tag{17}$$

are displayed in comparison with the corresponding force theorem results for the case of double layers of Fe separated by 13 layers of Au and $R = C_2$. For this particular system the force theorem calculation and the total energy calculation of

the MICE differ only by 0.009 mRy. As one can see from Fig. 7(a) the force theorem approximation yields a very smooth variation of the MICE with respect to layers, while the total energy approach yields comparatively large values of $\Delta\epsilon_i(R)$ for the two Fe layers and in the regime of the spacer. This strikingly different behavior becomes obvious looking at Fig. 7(b), showing the layer-resolved charges, Eq. (16). Now the force theorem values are rather large in the vicinity of the Fe layers. These difference charges in turn would cause differences in the layer-resolved Madelung potentials (see Ref. 10) in a self-consistent procedure, which ultimately are responsible for the oscillatory behavior of $\Delta\epsilon_i(R)$ in Fig. 7(a). Finally in Fig. 7(c) the differences of the magnetic moments, Eq. (11), are displayed. Quite clearly the force theorem values of $\Delta m_i(R)$ differ substantially from the corresponding values obtained within the total energy approach. Although the calculated MICE is almost identical in both calculations, local quantities such as layer-resolved charges and magnetic moments are remarkably different. It should be noted that in all cases investigated the same characteristic differences between the force theorem and the total energy calculations occur. This kind of difference one has to keep in mind when it comes to calculating transport properties, i.e., once attempts are made to calculate the giant magnetoresistance (GMR) in multilayer systems. It very well might turn out that in order to describe the GMR reasonably well, corresponding input data for a Kubo-Greenwood type description[13,14] have to be derived from a total energy approach.

V. CONCLUSION

In principle a spin-polarized relativistic approach is capable of describing correctly any noncollinear magnetic structure by providing automatically the appropriate symmetry constraints. It should be noted that by applying, for example, the torque method (see, e.g., Ref. 5) (i.e., by using a tensorial representation of spin and configuration for the Hamiltonian or the Green's function *without spin-orbit* coupling) rotations around the z axis (perpendicular to the planes) are infinitesimal. Such an approach, although quite useful in expressing the MICE in powers of the cosine of a relative angle, suffers from a lack of physical significance of the involved quantities, since such an angle neither refers to a well-defined relative spin orientation nor to a well-defined relative orientation of the magnetization.

In the present paper, which deals with simple configurations of different orientations of the magnetization in different layers of a multilayer system in terms of the spin-polarized relativistic screened KKR method, even a global relative angle describing relative orientations of the magnetization is physically meaningful and well defined. Furthermore, by using layer-resolved quantities very detailed information about the MICE can be obtained, which by going beyond the frozen potential or force theorem approximation hopefully will permit one to perform also direct calculations of the giant magnetoresistance and/or the magneto-optical properties.

ACKNOWLEDGMENTS

This paper was supported by the Austrian Ministry of Science (GZ. 45.368/2-IV/6/94) and the Austrian National Bank (P4648) and has benefited from collaborations within HCM-Network Contract No. ERBCHRXCT930369. Two of us (L.S. and B.U.) are also indebted to the Hungarian National Scientific Research Foundation for partial financial support (OTKA F014378). We also wish to thank the computing center IDRIS at Orsay as part of the calculations was performed on their Cray 98 machine.

[1] J. Unguris, R.J. Celotta, and D.T. Pierce, J. Appl. Phys. **75**, 6437 (1994).

[2] J. Kudrnovský, V. Drchal, I. Turek, and P. Weinberger, Phys. Rev. B **50**, 16 105 (1994).

[3] J. Kudrnovský, V. Drchal, I. Turek, M. Šob, and P. Weinberger, Phys. Rev. B **53**, 5125 (1996).

[4] P. Bruno, Phys. Rev. B **52**, 411 (1995).

[5] V. Drchal, J. Kudrnovský, I. Turek, and P. Weinberger, Phys. Rev. B **53**, 15 036 (1996).

[6] L. Szunyogh, B. Újfalussy, and P. Weinberger, Phys. Rev. B **51**, 9552 (1995).

[7] R. Feder and F. Rosicky, Z. Phys. B **52**, 52 (1983); P. Strange, J. Staunton, and B.L. Györffy, J. Phys. C **17**, 3355 (1984); A.C. Jenkins and P. Strange, J. Phys. Condens. Matter **6**, 3499 (1994); S.C. Lovatt, B.L. Györffy, and G.Y. Guo, *ibid.* **5**, 8005 (1993).

[8] P. Weinberger, *Electron Scattering Theory for Ordered and Disordered Matter* (Clarendon Press, Oxford, 1990).

[9] In a forthcoming paper it will be shown in terms of group theory that these rotation are related to the rotational invariance group of the Hamiltonian in Eq. (1).

[10] L. Szunyogh, B. Újfalussy, P. Weinberger, and J. Kollár, Phys. Rev. B **43**, 2721 (1994).

[11] L. Szunyogh, B. Újfalussy, P. Weinberger, and J. Kollár, J. Phys. Condens. Matter **6**, 3301 (1994).

[12] P. Bruno and C. Chappert, Phys. Rev. Lett. **67**, 1602 (1991).

[13] J. Banhart, H. Ebert, P. Weinberger, and J. Voitländer, Phys. Rev. B **50**, 2104 (1994).

[14] W.H. Butler, X.-G. Zhang, and D.M. Nicholson, J. Appl. Phys. **76**, 6808 (1994).